

Coherent diffusive transport mediated by Andreev reflections at $V = \Delta/e$ in a mesoscopic superconductor/semiconductor/superconductor junction

J. Kutchinsky

Niels Bohr Institute, University of Copenhagen, Universitetsparken 5, DK-2100 Copenhagen Ø, Denmark

R. Taboryski

Department of Physics, Technical University of Denmark, Building 309, DK-2800 Lyngby, Denmark

O. Kuhn

*Niels Bohr Institute, University of Copenhagen, Universitetsparken 5, DK-2100 Copenhagen Ø, Denmark
and Department of Physics, Chalmers University of Technology, University of Gothenburg, S-412 96 Gothenburg, Sweden*

C. B. Sørensen, P. E. Lindelof, and A. Kristensen

Niels Bohr Institute, University of Copenhagen, Universitetsparken 5, DK-2100 Copenhagen Ø, Denmark

J. Bindslev Hansen, C. Schelde Jacobsen, and J. L. Skov

Department of Physics, Technical University of Denmark, Building 309, DK-2800 Lyngby, Denmark

(Received 28 April 1997)

We present experiments revealing a singularity in the coherent current across a superconductor/semiconductor/superconductor (SSmS) junction at the bias voltage corresponding to the superconducting energy gap $V = \Delta/e$. The SSmS structure consists of highly doped GaAs with superconducting electrodes of aluminum configured as an interferometer. The phase-coherent component of the current is probed as the amplitude of $h/2e$ vs magnetic-field oscillations in the differential resistance of the interferometer. [S0163-1829(97)50234-7]

On the microscopic level the superconducting proximity effect, by which a superconducting order parameter is induced in a normal conductor (N) in contact with a superconductor (S), may be described in terms of Andreev reflections at the N - S boundary. In the dirty limit the decay length for the order parameter in the normal conductor is given by $\xi_N = \sqrt{\hbar D/2\pi k_B T}$ (with $\xi_N \gg l$), where l is the mean-free path. In a three-dimensional conductor with Fermi velocity v_F the diffusion constant is given by $D = 1/2v_F l$. However, even beyond ξ_N purely resistive corrections to the proximity effect may survive.¹

In superconductor-normal-metal-superconductor (SNS) or superconductor-semiconductor-superconductor (SSmS) structures with high transparency of the interfaces there is a high probability for multiple Andreev reflections, where the retroreflected electrons and holes may traverse the normal region several times. In the differential resistance vs bias voltage curves this effect gives rise to a subharmonic energy gap structure (SGS) at dc bias voltages $V = \pm 2\Delta/ne$, with $n = 1, 2, 3, \dots$, which for n traversals is the condition for maximum quasiparticle transfer through the normal region.^{2,3} Multiple Andreev reflections rely on energy conservation during the traversals of the normal conductor. This is clearly fulfilled in a ballistic system where in addition the phase of the traversing wave packet is practically unaltered. In a diffusive normal conductor the $2E$ energy difference between the incoming and the reflected particle will give rise to a phase difference in their wave functions. After diffusing an average length L in a conductor with diffusion constant D ,

the accumulated phase difference will amount to $\delta\phi = 2EL^2/\hbar D$. For a phase shift of 2π this defines a characteristic correlation energy $E_c = \hbar D/2L^2$. A more rigorous analysis yields $E_c = \hbar D/L^2$ for the effective correlation energy (also called the Thouless energy), which we shall use in the rest of this paper.

In a system with a normal conductor connected to two superconductors a strong dissipationless Josephson current may flow between the superconductors if the distance between the superconductors is smaller than or comparable to ξ_N . On a longer length scale the coupling will be too weak to lock the condensate phases of the two superconductors together, yet Andreev reflections with small excitation energy differences between incoming and outgoing quasiparticles may still impose resistive but phase-coherent transport in a mesoscopic normal conductor. The ultimate length scale over which such effects can survive is the phase-breaking diffusion length l_ϕ , which may be considerably longer than ξ_N . In many systems l_ϕ is limited by the inelastic scattering length (l_{in}) and hence in addition sets the cutoff length for the SGS as shown in Ref. 4. During the last five years this mesoscopic regime has generated increasing interest with emphasis on phase-coherent phenomena observed in normal conductors in contact with superconductors where a phase difference is imposed between two externally interconnected superconducting electrodes.⁵⁻¹² In Refs. 8 and 9 measurements on a flux-sensitive interferometer revealed the presence of quasiparticle interference at finite bias voltages in

addition to the well-known dc Josephson effect in a superconducting quantum interference device SQUID. However, in this case no SGS was observed and so far no experimental work on diffusive SNS structures has addressed the connection between phase-coherent transport and the SGS.¹³

In this work we present observations of phase-coherent transport at a dc voltage bias $V = \Delta/e$ in addition to zero bias in a diffusive SSMS magnetic-flux-sensitive interferometer. We have measured the oscillations in dV/dI as a function of applied magnetic field for a range of dc bias voltages, and found clear peaks in the oscillation amplitude centered around $V = 0$ and $V = \Delta/e$, while within the detection limit of our setup no oscillations were observed at other voltages, including $V = 2\Delta/e$. We would like to emphasize that our devices showed no supercurrent at temperatures down to 0.3 K. The effects studied here are therefore exclusively coherent transport phenomena due to quasiparticle interference in the normal conductor.

Our samples consisted of a 200-nm heavily doped GaAs (conduction channel) layer grown by molecular-beam epitaxy (MBE) on an insulating GaAs substrate. The GaAs is capped *in situ* (without breaking the vacuum) with 200 nm Al. The *in situ* Al deposition ensures a very smooth and clean interface. In order to increase the transparency of the Al/GaAs interface, five δ -doped layers were incorporated into the GaAs just under the Al cap layer. This had the effect of compensating the otherwise naturally formed Schottky barrier between Al and GaAs. The interface transparency was estimated to be $T \approx 0.5$. A 18- μm -wide Hall bar mesa pattern was etched in the Al/GaAs structure. The low-temperature mobility of the conductive GaAs layer was $\mu = 0.13 \text{ m}^2/\text{V s}$. The carrier density was $n_e = 4.8 \times 10^{24} \text{ m}^{-3}$, corresponding to a mean-free path of $l_0 \approx 50 \text{ nm}$ and a diffusion constant $D = 0.016 \text{ m}^2/\text{s}$. The Al film had a critical temperature equal to the bulk value $T_c = 1.2 \text{ K}$, and a superconducting energy gap $\Delta(0.3 \text{ K})/e \approx 167 \mu\text{V}$, close to the bulk value $\Delta(0) = 175 \mu\text{V}$. The details of the sample preparation are given in Ref. 14. The two sample layouts (I and II) shown in Fig. 1 are realized by pattern transfer using conventional electron-beam lithography followed by wet etching of the Al top layer. The geometry of our samples is similar to a dc SQUID, but no Josephson effect is observed. All samples investigated (both type I and II) were cut from the same wafer but processed individually. The phase-breaking diffusion length was determined independently from the weak localization magnetoresistance of the GaAs.⁴ At 0.3 K we found $l_\phi \approx 2.8 \mu\text{m}$. For $L \approx 1 \mu\text{m}$ our samples are therefore truly mesoscopic in the sense that $l \ll L < l_\phi$. The theoretical value of the coherence length at 0.3 K is $\xi_N = 250 \text{ nm}$. Most of the measurements were carried out on type-I samples. Here one of the superconducting Al electrodes is configured as an open superconducting loop (slit width $\approx 1 \mu\text{m}$). The superconducting counterelectrode is placed only $1 \mu\text{m}$ from the slit. This gives a correlation energy of $E_c = \hbar D/L^2 = 10.4 \mu\text{eV}$, corresponding to a temperature of $E_c/k_B = 0.12 \text{ K}$. Our measurements were carried out in a ^3He cryostat with a base temperature of 0.3 K.

In the structure sketched in Fig. 1 (type-I sample) the transport of quasiparticles from the counterelectrode to the slit electrode across the N region is probed as a function of the phase difference across the slit. The phase-coherent part

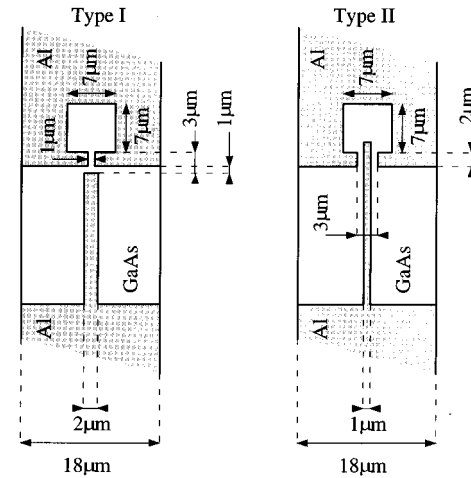


FIG. 1. Layout of the two types of interferometers used in the experiment. Only the central parts of the devices are shown, i.e., the contacts are not shown. Only devices of type I showed oscillations.

of the current is distinguished from the background current by application of a magnetic field perpendicular to the split loop electrode, which imposes a phase difference between the superconducting condensates on the two sides of the slit. During Andreev reflections at the two sides of the split Al electrode the quasiparticles are phase shifted by $\pm \phi_{1,2}$, the phase of the superconducting condensate. If an electronlike quasiparticle in this way is reflected from both parts of the split Al electrode, it undergoes a phase shift given by the phase difference $\phi_2 - \phi_1$ across the slit. This phase shift is modulated by 2π for each $h/2e$ quantum of magnetic flux applied through the loop. The oscillations in the dV/dI as a function of magnetic field at zero dc voltage bias are shown

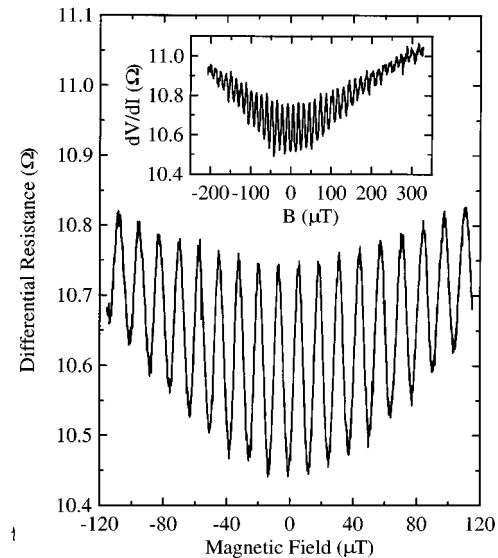


FIG. 2. Differential resistance vs applied magnetic field measured at zero bias voltage. The maximum oscillation amplitude is $\approx 70R_0e^2/h$. The inset shows a faster B -field sweep over a wider range. The oscillations die out at about $300 \mu\text{T}$, corresponding to an area of roughly $A = \Phi_0/300 \mu\text{T} \approx 2.5 \times 2.5 \mu\text{m}^2$. The measurement was carried out at 0.3 K on a type-I sample.

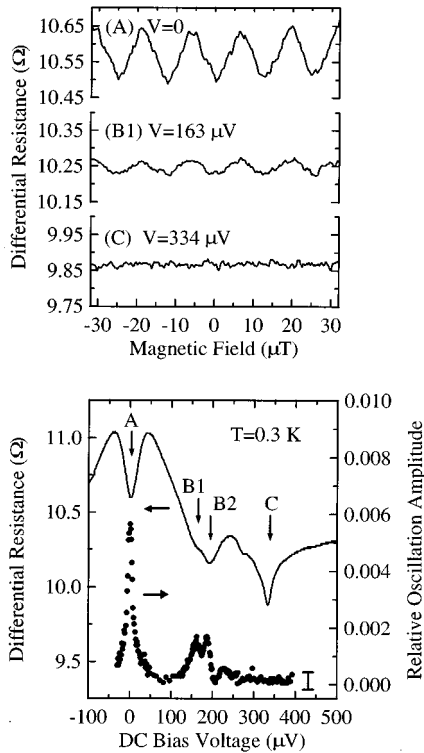


FIG. 3. Top panel: Differential resistance vs magnetic field at three dc bias voltages. Within our detection limit the $V=2\Delta/e$ curve showed no oscillations. Bottom panel: The differential resistance vs dc bias voltage at zero magnetic field, with indications of bias positions where the oscillations shown in the top panel were measured. The peak centered around $V=\Delta/e$ consists of two maxima denoted by B1 and B2. In the top panel only the oscillations at B1 are shown. The measurements were taken for the same device as in Fig. 2. The smaller amplitude of the oscillations is due to the extra noise added in the more complicated setup with a dc voltage bias. The fitted relative oscillation amplitude $\Delta(dV/dI)/(dV/dI)$ (see text) vs dc bias voltage is also shown. The error bar at the bottom right corner shows the estimated uncertainty of the fitting procedure.

in Fig. 2. The oscillation period is $\Delta B = 12.9 \times 10^{-6} T$, corresponding to one $h/2e$ flux quantum through an effective area of $\approx 12.7 \times 12.7 \mu\text{m}^2$, a factor of ≈ 3.2 larger than the nominal area shown in Fig. 1, but reasonable if one takes into account the flux focusing due to the expulsion of flux from the surrounding Al film (the Meissner effect). From symmetry considerations (of the envelope magnetic-field dependence) we found zero field to lie at a minimum in the oscillations (due to hysteresis in our superconducting solenoid zero applied field did not correspond to zero current through the coil). The maximum peak-to-peak oscillations amplitude is $\Delta R \approx 70R_0^2 e^2/h = 0.3 \Omega$, with $R_0 \approx 10 \Omega$. The amplitude is very sensitive to perturbations. The oscillation amplitude goes to zero when the ac excitation voltage exceeds 1–5 μV . In all measurements we used an ac excitation voltage so small that the oscillations amplitude did not depend on the ac voltage, and had room temperature π filters (20 dB loss at 600 kHz) on all sample leads.

For comparison we made samples with an alternative layout, shown as type II in Fig. 1. These samples differed from type-I samples in the sense that they had no common area

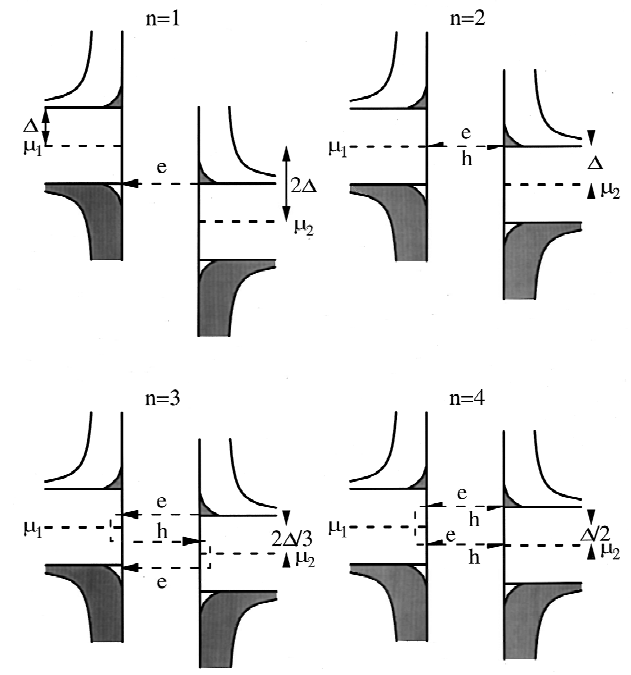


FIG. 4. Semiconductor representation of the density of states at finite temperature in the two superconductors in our SSmS structure for dc bias conditions corresponding to the first four multiple Andreev reflection processes ($n=1,2,3,4$). The shading shows the states occupied by electrons. At the gap energy there is a discontinuity in the density of states and a peak in the probability for Andreev reflection. For even n , quasiparticle interference may be enhanced (see text). The quasiparticle trajectories are shown with an electronlike particle traversing the first path; however time-reversed trajectories are equally possible (not shown).

shared between the split electrode and the counter electrode. For these samples we anticipated seeing no quasiparticle interference. We investigated two samples of type II, and found almost identical dV/dI vs V characteristics to those found for type-I samples, but indeed we observed no oscillations of the differential resistance as a function of magnetic field. We have investigated two samples of type I. Both showed similar results with well-pronounced oscillations in dV/dI vs magnetic field.

In Fig. 3 we present the main result of this paper. At zero bias and at $V=\pm\Delta/e$, $\pm 2\Delta/e$ we observe clear dips in the differential resistance as also reported previously.^{4,14} This behavior is shown in the bottom panel of Fig. 3. The SGS gradually disappears as the temperature approaches 1.2 K, the transition temperature of Al. This behavior is reported previously for the dV/dI vs V dependence in a simple geometry.¹⁴ The $\pm\Delta/e$ dip corresponds to two traversals of the normal region, first by an electronlike particle (or holelike particle) and then by an Andreev retroreflected holelike particle (or electronlike particle), while the $\pm 2\Delta/e$ dip corresponds to a single traversal of the normal region with no Andreev reflection. At zero bias and at $V=\Delta/e$ we observe well-pronounced oscillations in dV/dI vs B , but no oscillations at $V=2\Delta/e$. This is shown in the top panel of Fig. 3. The bottom panel shows the corresponding dV/dI vs V curve, and the oscillation amplitude in a broad range of bias voltages. The latter curve was obtained by fitting a sine function

to the data using a fixed field period and the relative amplitude as a fitting parameter.¹⁵ We see that the peak in the amplitude at $V=\Delta/e$ really consists of two separate maxima at $V=163\ \mu\text{V}$ and at $V=192\ \mu\text{V}$ denoted, respectively, by $B1$ and $B2$. This splitting is also observed (although less clearly) in the dV/dI vs V characteristics, and is present for all investigated samples with different layouts but only for interelectrode distances $\approx 1\ \mu\text{m}$. This splitting of the peak at $V=\Delta/e$ is not fully understood and is the subject of further studies.

The observation of a peak in the amplitude of the conductance oscillations with magnetic flux through the interferometer loop at $V=\Delta/e$ in Fig. 3 can be understood in qualitative terms: At a given bias voltage the peak shows up as a result of a simultaneous presence of coherence of an Andreev-reflected electron-hole pair moving across the semiconductor region and a peak in the quasiparticle density of states at the other interface. This is illustrated in Fig. 4 ($n=2$) and corresponds to the condition for observation of the conductance peak at $V=\Delta/e$, i.e., one of the peaks in the SGS. For a ballistic system the SGS was long ago² explained as a result of multiple Andreev reflections. This model is still roughly applicable for a diffusive normal conductor as in our case,⁴ if one includes a distinction between the energy-conserving diffusive transport across the semiconductor (the well-known multiple Andreev reflection model) and transport, which is furthermore enhanced by the coherence of the Andreev-reflected electron-hole pair, when the energy of the electron and the hole differs by less than the correlation energy $E_c=\hbar D/L^2$ ($\approx 10\ \mu\text{eV}$ for our samples). Using the semiconductor representation we may draw the density of states versus energy diagrams for $V=2\Delta/ne$ ($n=1,2,3,4$) as

seen in Fig. 4. The SGS minima seen in the dV/dI vs V curves are usually accounted for by the opening and closing of Andreev channels at $V=2\Delta/ne$, where the peaks in the density of states on both sides are involved in the transmission process. As seen, the $n=2$ and the $n=4$ are special in the sense that the singularity in the density of states coincides with a phase-correlated channel for an electron-hole pair. This phase correlation will only be maintained if the Andreev reflection takes place within E_c of the Fermi level on that particular side of the interferometer. In our experiment we observe for the first time separately this coherent part of the transmission as a peak in the amplitude of the conductance oscillations as a function of magnetic field at $V=2\Delta/2e$. We do not observe a similar peak at $V=2\Delta/4e$ because here the sum of four traversals of the normal region exceeds the phase-breaking diffusion length $l_\phi\approx 2.8\ \mu\text{m}$ (at 0.3 K) for our devices.

In conclusion, we have made observations of quasiparticle interference at a dc voltage bias $V=\Delta/e$ (in addition to zero bias) in a diffusive SSmS magnetic-flux-sensitive interferometer. We have measured the oscillations in dV/dI as a function of applied magnetic field for a range of dc bias voltages and found clear peaks in the oscillation amplitude centered around $V=0$ and $V=\Delta/e$, while within our detection limit (of roughly 20 m Ω on 10 Ω in the present setup) no oscillations were observed at other voltages including $V=2\Delta/e$.

We acknowledge useful discussions with Professor Anatoly Volkov and Professor Henrik Smith. This work was supported by the Danish Technical Research Council. We also thank CNAST for support and the III-V Nanolab at the Niels Bohr Institute for providing us with processing facilities.

¹A. Kastalsky *et al.*, Phys. Rev. Lett. **67**, 3026 (1991); Chang Nguyen *et al.*, *ibid.* **69**, 1416 (1992); and recent theory, for example, by Y. V. Nazarov and T. H. Stoof, *ibid.* **76**, 823 (1996); A. F. Volkov *et al.*, J. Phys.: Condens. Matter **8**, L45 (1996).

²P. E. Lindelof, Rep. Prog. Phys. **44**, 949 (1981); T. M. Klapwijk *et al.*, Physica B & C **109-110B+C**, 1657 (1982); M. Octavio *et al.*, Phys. Rev. B **27**, 6739 (1983); K. Flensberg *et al.*, *ibid.* **38**, 8707 (1988).

³W. M. van Hufelen *et al.*, Phys. Rev. B **47**, 5170 (1993).

⁴J. Kutchinsky *et al.*, Phys. Rev. Lett. **78**, 931 (1997).

⁵H. Courtois *et al.*, Phys. Rev. Lett. **76**, 130 (1996).

⁶P. G. N. de Vegvar *et al.*, Phys. Rev. Lett. **73**, 1416 (1994).

⁷H. Pothier *et al.*, Phys. Rev. Lett. **73**, 2488 (1994).

⁸A. Dimoulas *et al.*, Phys. Rev. Lett. **74**, 602 (1995).

⁹V. T. Petrashov *et al.*, Phys. Rev. Lett. **74**, 5268 (1995).

¹⁰S. G. den Hartog *et al.*, Phys. Rev. Lett. **76**, 4592 (1996).

¹¹P. Charlat *et al.*, Phys. Rev. Lett. **77**, 4950 (1996).

¹²S. G. den Hartog *et al.*, Phys. Rev. Lett. **77**, 4554 (1996).

¹³The importance of multiple Andreev reflections for the Josephson coupling has been treated theoretically, for example, by E. N. Bratus *et al.*, Phys. Rev. Lett. **74**, 2110 (1995); D. Averin and A. Bardas *ibid.* **75**, 1831 (1995).

¹⁴R. Taboryski *et al.*, Appl. Phys. Lett. **69**, 656 (1996).

¹⁵We used the Levenberg-Marquardt method. See W. H. Press, S. A. Teukolsky, W. T. Vetterling, and B. P. Flannery in *Numerical Recipes in C*, 2nd ed. (Cambridge University Press, Cambridge, 1992), pp. 681–688.